Journal of Marine Science and Technology

Volume 23 | Issue 5 Article 10

# NUMERICAL MODELLING OF THE WAVE PROPAGATION CLOSE TO THE SACALIN ISLAND IN THE BLACK SEA

Liliana Rusu
*Department of Mechanical Engineering, 'Dunărea de Jos' University of Galati, Romania.*, lrusu@ugal.ro

Dorin Butunoiu
*Department of Mechanical Engineering, 'Dunărea de Jos' University of Galati, Romania.*

# NUMERICAL MODELLING OF THE WAVE PROPAGATION CLOSE TO THE SACALIN ISLAND IN THE BLACK SEA

## Acknowledgements

This work was carried out in the framework of a grant from the Ministry of National Education, CNCS - UEFISCDI, project number PN-II-ID-PCE-2012-4-0089 (project DAMWAVE). The second author also acknowledges the receipt of a postdoctoral fellowship in the framework of the SOP-HRD project PERFORM (ID 138963). Finally, the authors would like to thank to Dr. Florin Tatui from the Faculty of Geography, University of Bucharest for providing some of the nearshore bathymetric data, and also for some outputs related to his in situ observations in the target area.

*Journal of Marine Science and Technology, Vol. 23, No. 5, pp. 669-677 (2015)*
DOI: 10.6119/JMST-015-0521-2


# NUMERICAL MODELLING OF THE WAVE PROPAGATION CLOSE TO THE SACALIN ISLAND IN THE BLACK SEA

Liliana Rusu and Dorin Butunoiu

Key words: wave modelling, SWAN, Black Sea, Sacalin Island, coastal changes.

## ABSTRACT

The target area of the present work is the nearshore neighbouring the Sacalin Island in the Black Sea, right off the Danube Delta and close to the Saint George branch of the Danube River. Being a newly formed island, this is a very special coastal environment. Moreover, because it has a great variety of rare fauna, the area was declared as an ecological reserve. A multilevel wave modelling system, based on the Simulating Waves Nearshore (SWAN) spectral model, was focused on the target area. In the final computational domain, with the highest resolution in the geographical space, the effect of the current induced by the Danube River outflow was also accounted for in the modelling process. The wave propagation patterns characteristic to this side of the sea, together with some parameters related to the shoreline conditions, were evaluated. Four different case studies were considered for a detailed analysis. The results provided by the modelling system revealed two antagonist processes. The first process, which is dominant, and that can be defined as a constructive process, corresponds to the waves coming from the northeast. The second process, which can be defined as a destructive process, corresponds to the conditions of extremely strong storms with waves coming from the southeast. Although such situations are quite rare, they might occur however from time to time and this is actually the case that generated in the winter of 2013 a strong penetration of the waves through the Sacalin Island changing the coastal configuration.

## I. INTRODUCTION

Sacalin is a newly formed island in the Black Sea, right off the coast of the Danube Delta, South of the Saint George branch. Initially, Sacalin was made up of two smaller islands, Greater Sacalin (Sacalinu Mare) and Lesser Sacalin (Sacalinu Mic) but, in time, the two islands merged into one continuous landmass as illustrated by Fig. 1. The island has become now the habitat of a great variety of birds, mammals and reptiles, being the main area for nesting, feeding and wintering of many rare species. For this reason, the Romanian government has declared the area an ecological reserve and no settlement is permitted on the island.


**Fig. 1. The Sacalin Island, picture taken from Google maps.**

The coastal environments with such morphological characteristics, as those of the Sacalin Island, are often called spits. The spits are usually very dynamic accumulating forms attached at one end to the mainland appearing in general in places where sudden changes in the coast orientation are encountered (Dan et al., 2011). A crucial concept considered when studying the spit dynamics is represented by the coastline equilibrium, which is mainly controlled by the wave regime and the longshore sediment transport patterns (Bondar and Panin, 2001).

*Paper submitted 08/22/14; revised 04/17/15; accepted 05/21/15.* *Author for correspondence: Liliana Rusu (e-mail: lrusu@ugal.ro).*
*Department of Mechanical Engineering, 'Dunărea de Jos' University of Galati, Romania.*

Some recent studies related to the coastal dynamics in the Sacalin area (Ovejanu, 2012; Păunescu, 2012; Dan, 2013) proved that the island had a large movement in a relatively short period of time. In the north of the island, it can be noticed how the seaside has come together with the island generating thus a peninsula. Towards the south, the coastal dynamics seems to be even higher. Thus, the first part is moving from east to west, while in the most southern part of the island the tendency of the movement is from west to east. So far, these movements seemed to lead to the formation of a lake by linking the south of the island to the main coast.

Nevertheless, this evolution was recently perturbed, in the winter of 2013, when, after some strong and rather atypical storms (with the waves coming from Southeast while in the case of most of the strong storms the wave direction is from Northeast or from East), the waves penetrated through the Sacalin Island and practically the island was again broken in some more parts. This event seriously affected the very rare flora and fauna of this area.

From this perspective, taking also into account the enhanced ecological importance and the high dynamics of this environment, a better understanding of the wave propagation patterns near the Sacalin Island becomes an issue of extreme relevance. In this connection, the objective of the present work is to develop a computational framework based on numerical spectral phase averaged models that can provide reliable outputs concerning the wave propagation patterns close to the Sacalin Island. By using such computational environment, extended hindcast studies were performed and various wave propagation scenarios were analysed, providing in this way a realistic picture of the coastal wave impact and of its influence in the dynamics of this coastal area. More details concerning the implementation and the performances of the wave modelling system, SWAN based, in the Black Sea are given in Rusu and Ivan (2010).

Finally, it has to be highlighted that, as a further extent, such a wave prediction system based on numerical models may also allow a real time delivery of reliable nowcast and forecast products concerning the wave propagation and impact in the target area.

## II. METHODS AND MATERIALS

### 1. Theoretical Formulations Considered in the Spectral Wave Models

Third generation wave models solve the energy balance Eq. (1) that describes the evolution of the wave spectrum in time, geographical and spectral spaces (which is usually defined by the relative radian frequency $\sigma$ and the wave direction $\theta$):

$$\frac{DN}{Dt}=\frac{S}{\sigma} \tag{1}$$

The recent versions of the spectral wave models consider the action density spectrum ($N$) instead of the energy density spectrum. This is because in the presence of current action density is conserved whereas energy density is not. The action density is equal to the energy density ($E$) divided by the relative frequency ($\sigma$). Since SWAN (Booij et al., 1999) is the wave model considered in the present study, the discussion will be focused on the particularities of this model. For large-scale applications, the governing equation in SWAN is related to the spherical coordinates longitude ($\lambda$) and latitude ($\varphi$) and the action balance equation becomes:

$$\frac{\partial N}{\partial t}+\frac{\partial}{\partial \lambda}\dot{\lambda}N+\frac{1}{\cos\varphi}\frac{\partial}{\partial \varphi}\dot{\varphi}N\cos\varphi+\frac{\partial}{\partial \sigma}\dot{\sigma}N+\frac{\partial}{\partial \theta}\dot{\theta}N=\frac{S}{\sigma} \tag{2}$$

For coastal applications, the Cartesian coordinates are mostly used in the SWAN simulations and the action balance equation becomes:

$$\frac{\partial N}{\partial t}+\frac{\partial}{\partial x}\dot{x}N+\frac{\partial}{\partial y}\dot{y}N+\frac{\partial}{\partial \sigma}\dot{\sigma}N+\frac{\partial}{\partial \theta}\dot{\theta}N=\frac{S}{\sigma} \tag{3}$$

$S$, from the right hand side of the action balance equation, represents the source terms. In deep water, three components are significant in the expression of the total source term. They correspond to the atmospheric input ($S_{in}$), whitecapping dissipation ($S_{dis}$) and nonlinear quadruplet interactions ($S_{nl}$), respectively. Various parameterizations for these source terms are alternatively available in SWAN and tuneable coefficients were defined for each case. Besides these three terms, in shallow water additional source terms corresponding to phenomena like bottom friction ($S_{bf}$), depth induced wave breaking ($S_{br}$) and triad nonlinear wave-wave interactions ($S_{tr}$), may play an important role, and the total source becomes (SWAN team, 2013):

$$S=S_{in}+S_{dis}+S_{nl}+\underbrace{S_{bf}+S_{br}+S_{tri}+...}_{finite\ \ depth\ \ processes} \tag{4}$$

Although the SWAN model is not considered very appropriate for ocean scale simulations, the recent developments implemented in SWAN in relationship with the propagation scheme and with some physical processes make the model now very suitable for simulations at sub oceanic scales. Consequently, SWAN definitively represents at this moment the best choice for enclosed seas, as the Black Sea is. Moreover, in such environments SWAN presents the advantage that one single model can cover the full scale of the wave modelling process in a multi-level wave modelling system that can be focused on the most sensitive coastal areas.

### 2. SWAN Implementation and Model Validations in the Black Sea

The wave modelling system, SWAN based, was extensively tested considering a computational domain that covers the

entire Black Sea. Some significant results related to the implementation in the Black Sea basin of this modelling system are provided in Rusu and Ivan (2010) and in Rusu (2011).

Validations have been carried out against both in situ measurements and remotely sensed data (Butunoiu and Rusu, 2012; Rusu et al., 2014) and the wave predictions were found in general reliable, being also more accurate than those obtained using a WAM based (WAMDI group, 1988) modelling system as presented by Cherneva et al. (2008).

On the other hand, from the point of view of the wave modelling processes, the enclosed seas (as the Black Sea is) are a much more difficult environment than the open ocean. In fact, in the enclosed or semi enclosed seas, the performance of the wave models depend in a higher degree than in the ocean on the quality of the driving wind fields, which are in general less accurate in such environments due to the strong influence of the land (Cavaleri and Bertotti, 2006). Nevertheless, this problem can be partially solved by an increase of the wind field resolution. In this connection, Rusu et al. (2008; 2014) performed extended studies concerning the influence of the accuracy and resolution of the forcing wind fields on the wave model performance. Their results reveal very clearly that in the coastal environment, in general, but especially in the case of the enclosed seas, a higher resolution in the geographical space of the wind model can account better for the influence of the land and consequently can provide a better framework for the wave model and improve the wave predictions.

From this perspective, the wind field provided by NCEP-CFSR (United States National Centers for Environmental Prediction, Climate Forecast System Reanalysis, Saha et al., 2010) with a spatial resolution of 0.312° × 0.312° and a temporal resolution of 3 h was considered in the present work.

Thus, simulations for the seven-year period 1999-2005 have been carried out at the level of the entire Black Sea basin. In this time interval, validations have been performed against both satellite data and in situ measurements. Table 1 illustrates the significant wave height ($H_s$) statistics, SWAN model simulations against remotely sensed data in the Black Sea and the SWAN results against in situ measurements at the Gloria drilling unit corresponding to the total time and only to the wintertime, respectively. The Gloria drilling platform operates in the western sector of the Black Sea at a location where the water depth is about 50 m (29.57°E/44.52°N). The measurements were performed daily during the seven-year period considered at 6-h intervals, the percentage of valid data being about 92% and the technique developed by Makarinskyy et al. (2005) was considered to fill the gaps in the measurements. The statistical parameters considered are those commonly used to evaluate the wave model output, such as the mean error (*Bias*) computed as the difference between the average values of the simulated (*MedSim*) and observed (*MedObs*) data, the mean absolute error (*MAE*), the root mean square error (*RMSE*), the scatter index (*SI*) defined as the ratio of the standard deviation of the error to the mean observed values, the linear correlation coefficient (*R*) and the symmetric slope

**Table 1. $H_s$ statistics, SWAN model simulations against remotely sensed data in the Black Sea and SWAN results against in situ measurements at the Gloria drilling unit corresponding to the total time and only to the wintertime, respectively. The period considered is 1999-2005.**

| Param | Sat-Total | Sat-Winter | Gloria-Total | Gloria-Winter |
|---|---|---|---|---|
| MeanM | 1.05 | 1.24 | 0.98 | 1.14 |
| MeanS | 1.03 | 1.22 | 0.94 | 1.11 |
| Bias | -0.03 | -0.02 | -0.04 | -0.04 |
| MAE | 0.28 | 0.30 | 0.28 | 0.30 |
| RMSE | 0.38 | 0.42 | 0.39 | 0.43 |
| SI | 0.36 | 0.33 | 0.40 | 0.37 |
| R | 0.86 | 0.87 | 0.85 | 0.86 |
| S | 1.00 | 1.01 | 0.92 | 0.93 |
| N | 438794 | 232307 | 9738 | 5008 |

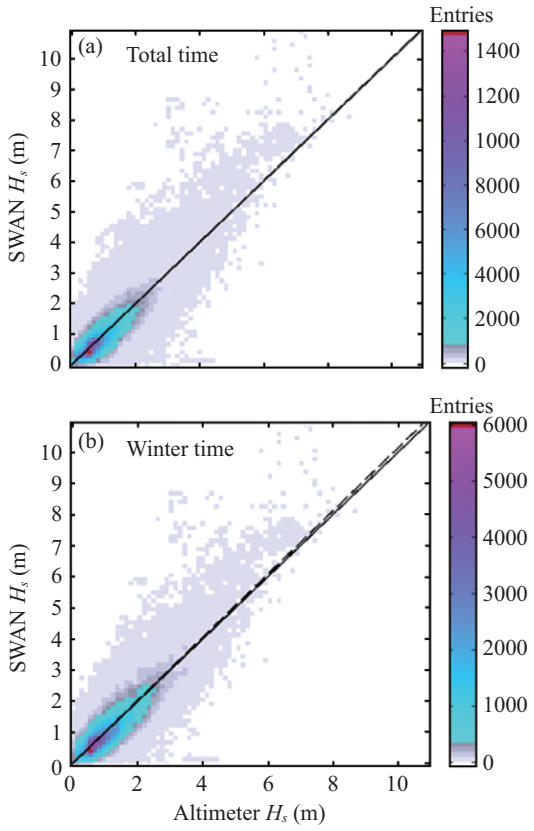


**Fig. 2. $H_s$ scatter diagrams, SWAN against satellite data in the Black Sea, results for the time interval 1999-2005. (a) the entire seven-year period; (b) wintertime.**

(*S*, for $S > 1$ the model overestimates the observations).

Fig. 2 illustrates the $H_s$ scatter diagrams, SWAN against the satellite data along the entire Black Sea basin, for the total seven-year period (a), and only for the winter time periods (b). In these analyses, the winter time represents all the periods

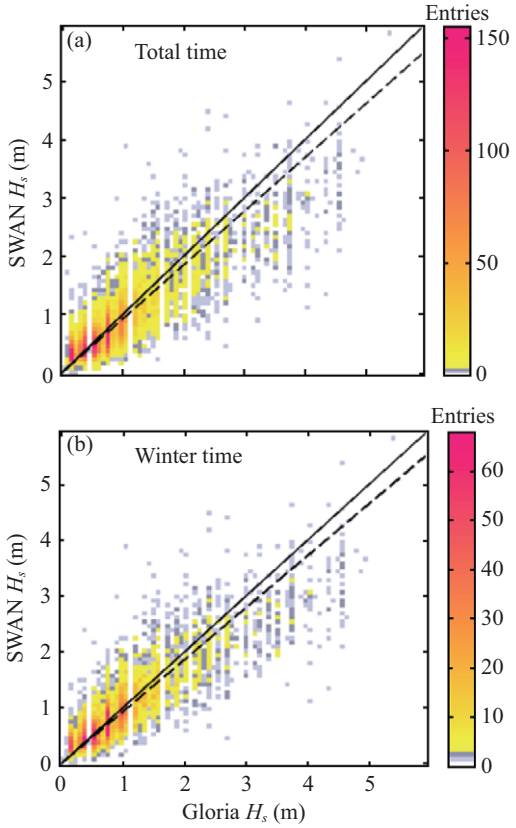


**Fig. 3. $H_s$ scatter diagrams, SWAN against in situ measurements carried out at the Gloria drilling unit in the Black Sea, results for the time interval 1999-2005. (a) the entire seven-year period; (b) winter-time.**

between September to March (inclusively). At the same time, Fig. 3 illustrates the $H_s$ scatter diagrams, SWAN against measurements at the Gloria drilling unit for the total seven-year period (a) and only for the winter time periods (b). The results presented in Table 1 and in Figs. 2 and 3 show that the computational framework developed herewith provides at a global scale reliable wave predictions. Moreover, these results are in line with the wave predictions provided in enclosed or semi enclosed seas by some others wave modelling systems (e.g. Bidlot et al., 2002; Ardhuin et al., 2007; Bertotti and Cavaleri, 2009). It has to be mentioned, however, that the above mentioned works are related to the Mediterranean and Adriatic seas, respectively, which are not enclosed seas.

Since the wave modelling system implemented for the entire Black Sea gives in general reasonable predictions, the next step is to focus this system in a multilevel scheme towards the target area, which is the Sacalin Island. For this purpose, two additional computational levels were considered. They are denoted as Level II, centred on the Danube mouths, representing also the area of the coastal wave transformation, and Level III defined in the coastal environment of the Sacalin Island, which represents the local area. The entire sea basin was also denoted as Level I, or the generation area. Nevertheless, it has to be highlighted that although one single wave model (SWAN) is considered for this system, the physics and model settings are rather different from one computational level to another. The characteristics of the three computational domains are presented in Table 2, while the corresponding physical processes activated in each computational level are in Table 3.

**Table 2. The computational grids considered in focusing the SWAN based modelling system towards the Sacalin coastal area. The quantities presented have the following significations: $\Delta x$ and $\Delta y$ - resolution in the geographical space, $\Delta\theta$ - resolution in directional space, $\Delta t$ - time step, *nf* - number of frequencies in the spectral space, $n\theta$ - number of directions in the spectral space, *ngx* - number of grid points in *x* direction, *ngy* - number of grid points in *y* direction, *np* - total number of grid points.**

| Level | I - Sea basin | II - Danube mouths | III - Sacalin |
|---|---|---|---|
| Coord. | Spherical | Spherical | Cartezian |
| $\Delta x \times \Delta y$ | 0.08° × 0.08° | 0.01° × 0.01° | 200 m × 200 m |
| $\Delta\theta \times \Delta t$ (°)-(min) | 10 × 20 | 10 × 20 | 10 × 20 |
| Mode | non-stat | non-stat | non-stat |
| *nf* | 30 | 30 | 30 |
| $n\theta$ | 36 | 36 | 36 |
| *ngx* × *ngy* = *np* | 176 × 76 = 13376 | 176 × 176 = 30976 | 353 × 251 = 88603 |

Fig. 4 presents the geographical spaces of the three computational domains having in the background the bathymetric map of each area. As it can be seen in this figure, while the first two computational domains (Levels I and II) are defined in spherical coordinates (longitude, latitude), at the final computational level (III) the Cartesian coordinates were considered. This is because some processes, as for example the wave induced set up, that might be relevant in the target area can be activated in SWAN only when the Cartesian coordinates are used. The position of the Gloria drilling unit is also represented in this figure.

This coordinate change introduces however an additional modelling difficulty because in such case the passage to the higher resolution computational level within the nesting procedure is not automatically performed and in order to achieve this transition nine reference points were defined on the boundary of the high resolution computational domain (Fig. 5(a)). The positions of these points were also defined in the spherical system and the corresponding wave spectra were requested as output during the simulations carried out in the second computational level. These spectral files were considered to provide variable boundary conditions in the final computational level. As an example, such a 2D wave spectrum is illustrated in a normalized form in Fig. 5(a).

**Table 3. SWAN model configurations for the three computational domains considered. The significations of the input fields and of the physical processes presented are: *wave* - wave forcing, *tide* - tide forcing, *wind* - wind forcing, *curr* - the current field input, *gen* - generation by wind, *wcap* - whitecapping process, *quad* - quadruplet nonlinear interactions, *triad* - triad nonlinear interactions, *diff* - diffraction process, *bfric* - bottom friction, *set up* - wave induced set up, *br* - depth induced wave breaking. The symbol X indicates that the process is activated, while the symbol 0 indicates that the respective process is not activated.**

| Level/ Input-proc | I - Sea basin | II - Danube mouths | III - Sacalin |
|---|---|---|---|
| *wave* | 0 | X | X |
| *wind* | X | X | X |
| *tide* | 0 | 0 | 0 |
| *curr* | 0 | 0 | X |
| *gen* | X | X | X |
| *wcap* | X | X | X |
| *quad* | X | X | X |
| *tri* | 0 | 0 | X |
| *diff* | 0 | 0 | X |
| *bf* | X | X | X |
| *set up* | 0 | 0 | X |
| *br* | X | X | X |

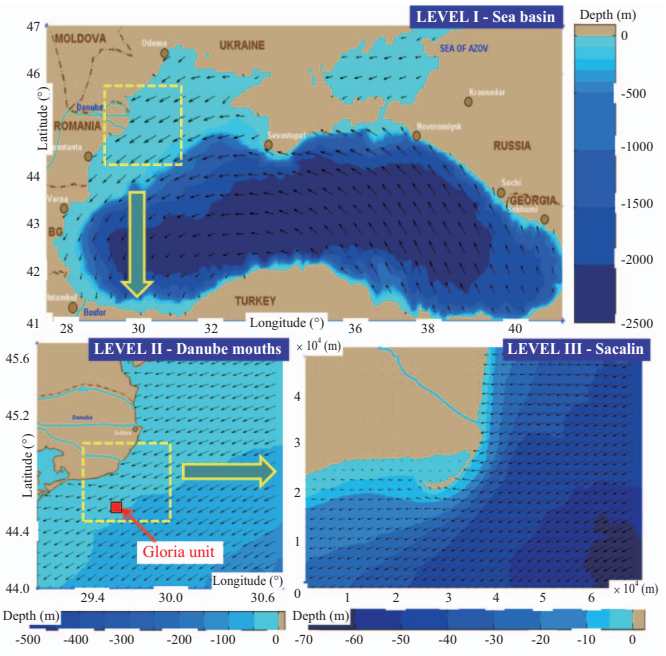


**Fig. 4. Focusing of the wave prediction system towards the Sacalin coastal area, bathymetric maps and wave vectors illustrating the dominant wave propagation pattern. The position of the Gloria drilling unit is also represented.**

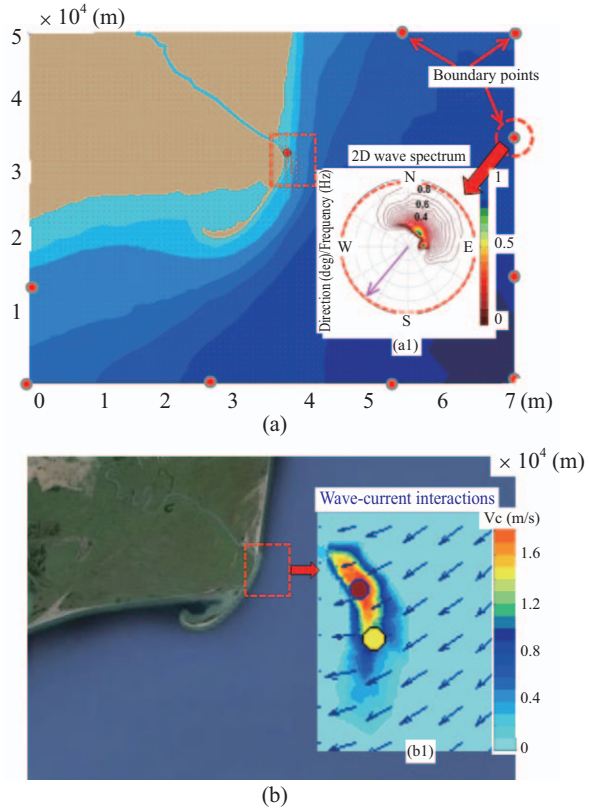


**Fig. 5. Wave modelling in the high resolution computational domain. (a) The boundary points defined to couple the Cartesian system to the spherical; (a1) 2D normalized wave spectrum. (b) The geographical space of the target area, (b1) Dominant pattern for a high energy situation, scalar current fields and wave vectors.**

Another important issue is related to the effect of the currents. The studies performed by Ivan et al. (2012) show that in general in the target area the marine currents do not have a significant influence on the wave propagation, since they are mainly following currents and they have also relatively small intensities.

On the other hand, the opposite currents induced by the Danube River outflow determine locally a significant enhancement of the incoming waves. The experimental studies performed by Rusu and Guedes Soares (2011) showed that the SWAN model is able to provide reliable results in relation with the interactions of the coastal waves with the strong opposite currents.

For this reason, based on various in situ measurements performed at the Saint George branch, three different scenarios of the current field were designed, corresponding to high, average and low flowing conditions, respectively. Since in fact the current intensity can be also controlled during the SWAN simulations via a scaling factor, this approach covers a large variety of flowing cases. In the case of the high flowing conditions, the current vectors are illustrated in Fig. 5(a), while the scalar current fields in Fig. 5(b). The red point in this figure indicates the location of the maximum current value and

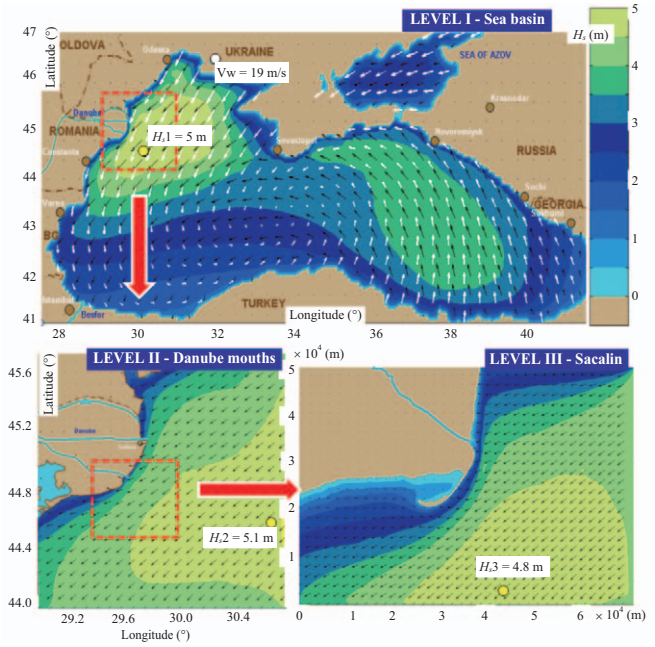


**Fig. 6. System focusing towards the Sacalin Island. Model results corresponding to the time frame 2002/03/25/h12 (high wave conditions in the target area), in background significant wave height scalar fields, in foreground wave vectors.**

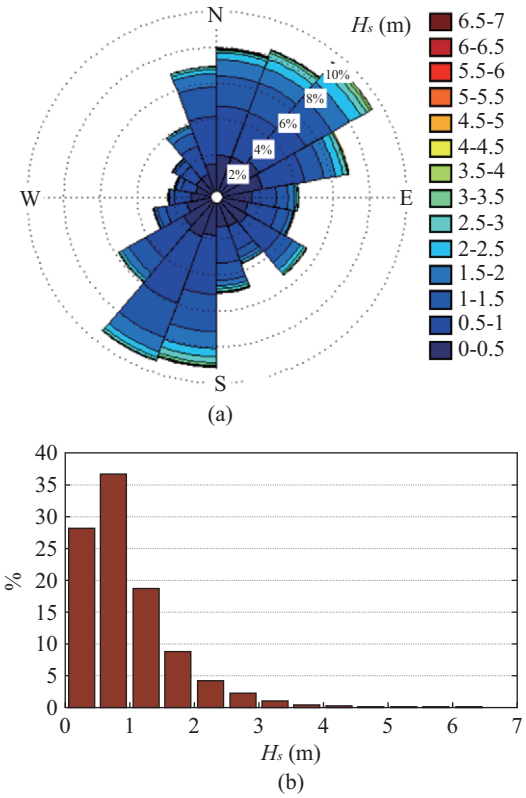


**Fig. 7. (a) The $H_s$ classes distributed for each directional bin of 10°, SWAN results in a location offshore the Sacalin Island (30.05°E, 44.77°N, close to the southeastern corner of the high resolution SWAN computational domain) for the time interval 1999-2005; (b) $H_s$ histogram corresponding to the same location and time interval.**

the yellow point the position of the maximum value of the significant wave height corresponding to the most common pattern of wave propagation, when the waves are coming from the northeast direction.

Following the above-mentioned approach, an effective computational framework based on the SWAN spectral phase averaged model was developed. This is focused on the coastal environment close to the Sacalin Island. As an example of this system focusing, model results corresponding to the time frame 2002/03/25/h12 (reflecting relatively high wave conditions in the target area with the waves coming from the northeast) are illustrated in Fig. 6. The background of this figure presents the $H_s$ scalar fields, while the foreground the wave vectors.

## III. RESULTS AND DISCUSSIONS

Fig. 7(a) illustrates the $H_s$ classes distributed for each directional bin of 20°, as resulted from the seven-year SWAN simulations (1999-2005). The results are reported to a location just offshore the Sacalin Island (30.05°E/44.77°N), close to the south-eastern corner of the high resolution SWAN computational domain. Corresponding to the same location and time interval, Fig. 7(b) presents the $H_s$ histogram. Based on these data, the wave conditions offshore the target area were analysed and the most relevant wave propagation patterns in the nearshore area close to Sacalin were defined together with some extreme scenarios. As a next step, following the above defined wave patterns specific to the coastal area targeted, four relevant case studies (CS) were considered for a more detailed analysis and they will be next presented and discussed. These are denoted as CSI to CSIV.

CSI corresponds to the situation when the waves come from the north (about 18 degrees in the nautical convention, which means the direction from where the waves are coming, measured from the geographic north) and significant wave heights on the external boundaries (N and E) between 2 m and 3 m. Such situation presents one of the most frequent cases of the wave propagation while the magnitude of the waves in terms of significant wave height is characteristic for the average to high winter time conditions.

Corresponding to this situation, the wind direction in the target area was 34 degrees and the velocity 7.2 m/s. Although this case study reflects the real conditions corresponding to the time frame 2003/04/07/h09, it has to be highlighted that this is in fact also a very common wave pattern that might be often encountered in the target area.

CSII presents an extreme situation that corresponds to the waves coming from the northeast (about 35 degrees in the nautical convention) and significant wave heights of about 7 m on the external boundary (E). The wind direction in the target area was about 22 degrees with intensity of 24.2 m/s. This

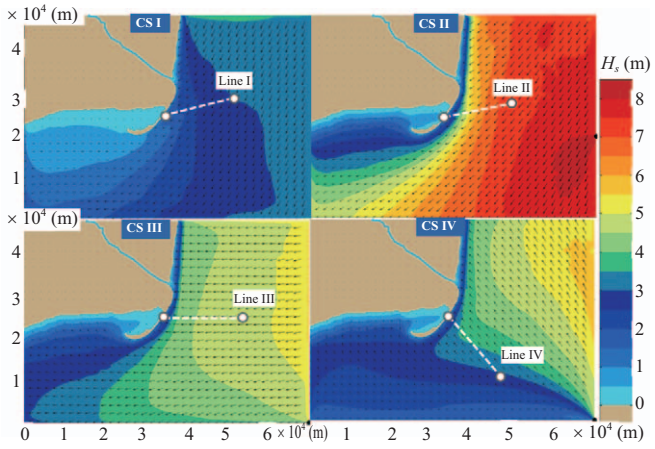


**Fig. 8. CSI-CSIV, wave propagation patterns in the target area. In background the significant wave height scalar fields are represented while in foreground the wave vectors. The positions of the reference lines defined for each case study are also illustrated.**

situation reflects the real conditions corresponding to the time frame 2004/22/01/h21, which represents also the highest energetic situation encountered in the western side of the Black Sea in the seven-year period analysed.

In the case denoted as CSIII, the waves come almost normal to the coast (about 82 degrees in nautical convention) and the significant wave height on the external boundary (E) is of about 5 m, conditions that in terms of significant wave height are characteristic to the normal winter storms. For this case study, the wind direction in the target area was of about 88 degrees and the wind velocity is 15.3 m/s. This case is also similar to the real conditions from the time frame 2004/01/17/h00.

Finally, CSIV illustrates the situation when the waves come from the southeast (about 155 degrees in the nautical convention). From an energetic point of view, this situation also corresponds to a normal winter storm with a significant wave height on the external boundary (E) slightly lower than 5 m. For this case study, the wind direction in the target area was 154 degrees and the wind velocity 14.6 m/s. This situation reflects the real conditions corresponding to the time frame 2002/03/24/h06 but is also rather similar (although had smaller values in terms of significant wave height) with the strong storm conditions from 2013 that penetrated the island.

Corresponding to these four case studies above described, Fig. 8 presents the wave propagation patterns in the target area, as given by the model simulations in the high-resolution computational domain. The background of the figure presents the scalar $H_s$ fields, while the foreground the wave vectors. For each case study, a reference line was defined following the direction of the wave propagation close to the coast. The positions of these reference lines are also illustrated in Fig. 8. The variations along the reference lines of the main wave parameters (significant wave height - $H_s$, group velocity, water depth and wave power) are illustrated in Fig. 9. In order to give a graphical representation of these data, each reference

**Table 4. SWAN results for the main wave parameters in the nearshore extremity (water depth 0.7 m) of the reference lines for CSI to CSIV.**

| Case/Param | $H_s$ (m) | $Dir$ (°) | $L$ (m) | $F$ (N) | $U_{bot}$ (m/s) | $V_{phase}$ (m/s) |
|---|---|---|---|---|---|---|
| CSI | 0.67 | 75.2 | 18 | 12.6 | 0.6 | 2.8 |
| CSII | 0.72 | 81.2 | 16 | 12.7 | 0.6 | 2.9 |
| CSIII | 0.75 | 91.7 | 18 | 13.4 | 0.7 | 3.1 |
| CSIV | 0.97 | 98.4 | 17 | 14.8 | 0.9 | 3.9 |

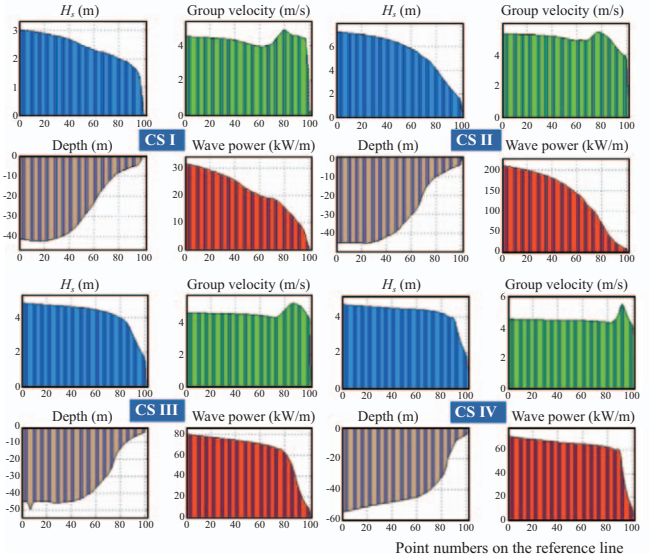


**Fig. 9. Variations along the reference lines, defined for the case studies considered (CSI-CSIV), of the main wave parameters (significant wave height - $H_s$, group velocity, water depth and wave power). The reference lines are divided in 100 points equally spaced.**

line was divided in 100 points equally spaced.

Finally, Table 4 presents the SWAN results for some relevant wave parameters in the nearshore extremity (water depth 0.7 m) of the reference lines for CSI to CSIV. The wave parameters presented in Table 4 are: significant wave height ($H_s$), mean wave direction ($Dir$), wavelength ($L$), wave force ($F$), the root-mean-square value of the maxima of the orbital motion near the bottom ($U_{bot}$) and the phase velocity ($V_{phase}$).

As discussed above, the most common pattern for the wave propagation in the target area is related to the waves coming from the northeast, these directions representing more than 50% of the total incoming waves (Fig. 7(a)). The strongest storms are also following this pattern. The model results presented in Figs. 8 and 9 and in Table 4 indicate that, due to the bathymetric particularities, for such wave conditions (waves coming from the northeast) both the wave refraction and dissipation are enhanced and even in the case of the extreme storms the wave energy is dissipated faster and the significant wave height decreases gradually before approaching the island. Such features are very well illustrated by the sig-

nificant wave height variations presented in Fig. 9 for CSI and CSII. On the other hand, for this oblique wave approach the nearshore wave induced currents pointing south are higher. These currents are the most important factor in driving the sediment transport. In fact, it appears quite obvious that this is the mechanism that determined the initial generation of the Sacalin Island and its extension towards the south. This is because in such case the wave induced nearshore currents interact with the currents generated by the Danube River outflow driving towards south the Danube sediment discharge.

From the point of view of the wave penetration through the island, the results show that the most dangerous are the waves coming from the southeast and also (to a lesser extent) the waves coming from the east (situations reflected by CSIV and CSIII). In such cases, even the regular storms can produce in the reference point waves with significant wave heights higher than 0.95 m. It has to be highlighted that since the reference point is in shallow water (0.7 m), in such situation the point will be located in the surf zone and, as illustrated by Fig. 9, in fact a significant wave height of above 4 m is estimated just before the breaking process to start, value which is considerably higher than in CSI and CSII when the process of wave energy dissipation initiates earlier. As illustrated also by Fig. 9, in CSIV the incoming wave power along a meter of wave front on the offshore extremity of the reference line is lower than in CSII or CSIII, being about 65 kW/m in CSIV against more than 80 kW/m or 200 kW/m, in CSIII and CSII respectively. Despite this, in CSIV not only the significant wave height appears to be considerably higher in the nearshore reference point considered for the present analysis (the nearshore extremity of the reference line), but also the other relevant parameters (group velocity, phase velocity, orbital velocity at the bottom and wave force) present significantly higher values. This demonstrates that a wave approach from the southeast is the most dangerous from the point of view of the wave penetration through the Sacalin Island.

## IV. CONCLUSION

The present work presents some results provided by a wave modelling system, based on the SWAN spectral phase averaged model that was focused on the nearshore area neighbouring the Sacalin Island. This is a very particular and important coastal environment, being a newly created Island.

Model system simulations have been performed considering the most relevant wave propagation patterns specific to this coastal environment. A first conclusion would be that the results provided by the modelling system developed herewith are in general in line with the outputs of the previous studies based mainly on observations and some in situ measurements and these model results directly help in both following and explaining the very dynamic coastal evolutions in the target area.

Thus, the model results reveal two antagonist processes. The first, which is dominant, and that can be defined as a constructive process, corresponds to the most common wave propagation pattern in the target area (that is the waves coming from the northeast). In this case, the alluvial river input, combined with the longshore sediment transport, determine the southern extension of the Sacalin Island. In fact, this was also the mechanism that determined the generation of the Sacalin Island more than one century ago. Corresponding to various moments of the evolution of the Sacalin system, field evidence concerning the dynamics of this coastal environment were made available in a large number of references from which we mention as more relevant: Bondar and Panin (2001), Dan et al. (2011), Ovejanu (2012), Păunescu (2012) and Dan (2013).

The second, who can be defined as a destructive process, is characteristic of the strong storm conditions with waves coming from the southeast (and to a lesser extent also from the east). Although the statistics presented in Fig. 7(a) show that more than 20% of the regular waves are following this pattern in terms of wave propagation, strongest storms coming from the southeast are less frequent and that is why the constructive process appears to be dominant, allowing the generation and the last decades spatial extension towards the south of the Sacalin Island. However, when the waves are coming from the southeast, they appear to be much stronger. Consequently, in the case of the most extreme storms following such a pattern, the waves can penetrate the island, sometimes destroying in only one day, years of sediment accumulations and putting in danger the very rare fauna living on the island. This was really happening in the winter of 2013.

Finally, it has to be also highlighted that a computational framework based on numerical wave models has been developed and described in the present work. Beside the more in situ validations, in order to improve locally the reliability of the wave predictions, some protection scenarios are also considered for the future work.

Thus, a viable solution to assure protection to the coastal environment of the Sacalin Island would be to install a marine energy park offshore the island. Such scenarios were already explored in the target area by Diaconu and Rusu (2013) considering a Wave Dragon based wave farm and by Zanopol et al. (2014), where a generic wave farm was considered together with various transmission scenarios. Since this is in fact one of the most energetic areas in the Black Sea's nearshore, such farm might become economically effective, especially as regards a hybrid wind-wave solution. Moreover, the results provided by the above mentioned studies show that a marine energy farm will decrease considerably the wave impact in the coastal environment and might provide an effective protection to the Sacalin Island.

Moreover, besides designing various scenarios and analyses, the wave prediction system developed in the present work allows the real time release of reliable nowcast and forecast products concerning the nearshore wave conditions at the mouths of the Danube River in the Black Sea, in general, and in the marine environment close to the Sacalin Island, in special.

## ACKNOWLEDGMENTS

This work was carried out in the framework of a grant from the Ministry of National Education, CNCS - UEFISCDI, project number PN-II-ID-PCE-2012-4-0089 (project DAMWAVE). The second author also acknowledges the receipt of a post-doctoral fellowship in the framework of the SOP-HRD project PERFORM (ID 138963). Finally, the authors would like to thank to Dr. Florin Tatui from the Faculty of Geography, University of Bucharest for providing some of the nearshore bathymetric data, and also for some outputs related to his in situ observations in the target area.

## REFERENCES

Ardhuin, F., L. Bertotti, J.-R. Bidlot, L. Cavaleri, V. Filipetto, J. M. Lefevre and P. Wittmann (2007). Comparison of wind and wave measurements and models in the Western Mediterranean Sea. Ocean Engineering 34(3-4), 526-541.

Bertotti, L. and L. Cavaleri (2009). Wind and wave predictions in the Adriatic Sea. Journal of Marine Systems 78, S227-S234.

Bidlot, J.-R., D. J. Holmes, P. A. Wittmann, R. Lalbeharry and H. S. Chen (2002). Intercomparison of the performance of operational ocean wave forecasting systems with buoy data. Weather and Forecasting 17, 287-310.

Bondar, C. and N. Panin (2001). The Danube Delta hydrologic database and modelling. Geo- Eco-Marina 5-6, 5-52.

Booij, N., R. C. Ris and L. H. Holthuijsen (1999). A third generation wave model for coastal regions. Part 1 - Model description and validation. Journal of Geophysical Research 104, 7649-7666.

Butunoiu, D. and E. Rusu (2012). Sensitivity tests with two coastal models. Journal of Environmental Protection and Ecology 13(3), 1332-1349.

Cavaleri, L. and L. Bertotti (2006). The improvement of modeled wind and wave fields with increasing resolution. Ocean Engineering 33(5-6), 553-565.

Cherneva, Z., N. Andreeva, P. Pilar, N. Valchev, P. Petrova and Guedes Soares (2008). Validation of the WAMC4 wave model for the Black Sea. Coastal Engineering 55, 881-893.

Dan, S. (2013). Coastal Dynamics of the Danube Delta. Ph.D. thesis, Delft University of Technology, Netherlands.

Dan, S., D. J. R. Walstra, M. J. F. Stive and N. Panin (2011). Processes controlling the development of a river mouth spit. Marine Geology 280, 116-129.

Diaconu, S. and E. Rusu (2013). The environmental impact of a Wave Dragon array operating in the Black Sea. The Scientific World Journal, ID 498013, 1-20.

Ivan, A., C. Gasparotti and E. Rusu (2012). Influence of the interactions between waves and currents on the navigation at the entrance of the Danube Delta. Journal of Environmental Protection and Ecology 13(3A), 1673-1682.

Makarynskyy, O., D. Makarynska, E. Rusu and A. Gavrilov (2005). Filling gaps in wave records with artificial neural networks. In: maritime transportation and exploitation of ocean and coastal resources, edited by Guedes Soares, C., Garbatov, Y. and Fonseca, N., Taylor & Francis Group, London, 1085-1091.

Ovejanu, I. (2012). Morphology and morphogenesis at the Saint George mouth (Danube Delta). Bucharest, Romania. (in Romanian)

Păunescu, C. (2012). A study of migration in time of the Sacalin Island, Danube Delta, Romania. Proceedings of the Romanian Academy, Series B 2, 156-160.

Rusu, E. (2010). Modeling of wave-current interactions at the Danube's mouths. Journal of Marine Science and Technology 15(2), 143-159.

Rusu, E. (2011). Strategies in using numerical wave models in ocean/coastal applications. Journal of Marine Science and Technology- Taiwan 19(1), 58-73.

Rusu, L., M. Bernardino and C. Guedes Soares (2008). Influence of the wind fields on the accuracy of numerical wave modelling in offshore locations. Proceedings of the 27th International Conference on Offshore Mechanics and Arctic Engineering, Estoril, Portugal, Vol 4, 637-644.

Rusu, L., M. Bernardino and C. Guedes Soares (2014). Wind and wave modelling in the Black Sea. Journal of Operational Oceanography 7(1), 5-20.

Rusu, L., D. Butunoiu and E. Rusu (2014). Analysis of the extreme storm events in the Black Sea considering the results of a ten-year wave hindcast. Journal of Environmental Protection and Ecology 15(2), 445-454.

Rusu, L. and C. Guedes Soares (2011). Modelling the wave-current interactions in an offshore basin using the SWAN model. Ocean Engineering 33(1), 63-76.

Rusu, L. and A. Ivan (2010). Modelling wind waves in the romanian coastal environment. Environmental Engineering and Management Journal 9(4), 547-552.

Rusu, E. and S. Macuta (2009). Numerical modelling of longshore currents in marine environment. Environmental Engineering and Management Journal 8(1), 147-151.

Saha, S., S. Moorthi, H. Pan, X. Wu, J. Wang, S. Nadiga, P. Tripp, R. Kistler, J. Wollen, D. Behringer, H. Liu, D. Stokes, R. Grumbine, G. Gayno, J. Wang, Y. Hou, H. Chuang, H. Juang, J. Sela, M. Iredell, R. Treadon, D. Kleist, P. Vandelst, D. Keyser, J. Derber, M. Ek, J. Meng, H. Wei, R. Yang, S. Lord, H. Van den Dool, A. Kumar, W. Wang, C. Long, M. Chelliah, Y. Xue, B. Huang, J. Schemm, W. Ebisuzaki, R. Lin, P. Xie, M. Chen, S. Zhou, W. Higgins, C. Zou, O. Liu, Y. Chen, Y. Han, L. Cucurull, R. Reynolds, G. Rutledge and M. Goldberg (2010). The NCEP climate forecast system reanalysis. Bulletin of the American Meteorological Society 91, 1015-1022.

SWAN team (2013). Scientific and technical documentation. SWAN Cycle III version 40.91, Delft University of Technology, Department of Civil Engineering, Netherlands.

WAMDI group (1988). The WAM model - a third generation ocean wave prediction model. Journal of Physical Oceanography 18, 1775-1810.

Zanopol, A., F. Onea and E. Rusu (2014). Coastal impact assessment of a generic wave farm operating in the Romanian nearshore. Energy 72(8), 652-670.